Dynamics and ultrastructure of developmental cell fusions in the *Caenorhabditis elegans* hypodermis

William A. Mohler*, Jeffrey S. Simske†, Ellen M. Williams-Masson*‡, Jeffrey D. Hardin† and John G. White*‡§

Cell fusions produce multinucleate syncytia that are crucial to the structure of essential tissues in many organisms [1–5]. In humans the entire musculature, much of the placenta, and key cells in bones and blood are derived from cell fusion. Yet the developmental fusion of cell membranes has never been directly observed and is poorly understood. Similarity between viral fusion proteins and recently discovered cellular proteins implies that both cell–cell and virus–cell fusion may occur by a similar mechanism [6–8]. Paradoxically, however, fusion of enveloped viruses with cells involves an opening originating as a single pore [9–11], whereas electron microscopy studies of cell–cell fusion describe simultaneous breakdown of large areas of membrane [12,13]. Here, we have shown that developmental cell fusion is indeed consistent with initiation by a virus-like, pore-forming mechanism. We examined live cell fusions in the epithelia of *Caenorhabditis elegans* embryos by a new method that integrates multiphoton, confocal, and electron microscopy. The fusion aperture always originated at a single point restricted to the apical adherens junction and widened slowly as a radial wavefront. The fusing membranes dispersed by vesiculation, rather than simple unfolding of the conjoined double bilayer. Thus, in these cells fusion appears to require two specialized sequential processes: formation of a unique primary pore and expansion of the opening by radial internalization of the interacting cell membranes.

Addresses: *Laboratory of Molecular Biology, †Department of Zoology, ‡Integrated Microscopy Resource, and §Department of Anatomy, University of Wisconsin, Madison, Wisconsin 53706, USA.

Correspondence: William A. Mohler
E-mail: wamohler@facstaff.wisc.edu

Received: 7 July 1998
Revised: 24 August 1998
Accepted: 24 August 1998

Published: 14 September 1998

Current Biology 1998, 8:1087–1090
http://biomednet.com/elecref/0960982200801087

Results and discussion

The timing of cell fusion events in the external epithelium (hypodermis) of *C. elegans* embryos is essentially invariant, as are the lineage, position, and geometry of participating cells, making this tissue amenable to reproducible observation of ongoing cell fusions within a live organism [4,14]. We followed the dynamics of cell membranes via automated time-lapse multiphoton laser scanning microscopy (MPLSM) [15] and four-dimensional reconstruction of live embryos labeled with the vital fluorescent membrane probe FM 4–64 [16,17]. By 400 minutes of development, precursors of the largest hypodermal syncytium, hyp7, covered the dorsal third of the embryo, aligning circumferentially such that approximately 50 to 60 μm^2 of each cell's lateral membrane was in contact with another flanking hyp7 progenitor (Figure 1a,b). The syncytium was formed by the disappearance of these lateral membranes in a sequence of cell fusions that agreed well with previous reports tracing the loss of apical adherens junctions in fixed embryos [14].

In optical cross-sections, the vanishing of membranes between two fusing cells always progressed in an apical-to-basal direction (Figure 1c). Through time-animated volume (stereo-four-dimensional) reconstruction [17], fusion was seen to originate at a site at the apical edge of the fusing border and to propagate both basally and along the length of the membrane, producing a single widening semi-elliptical aperture which first reached the basal edge of the lateral membranes and then progressed to the circumferential margins of the cells (Figure 1d). The rate of radial increase of the opening was 0.40 ± 0.33 μm per minute, measured in a total of 275 time increments in optical sections from 17 different fusion events in 9 recorded embryos. Elimination of the entire area of membrane interface between two neighboring cells required up to 30 minutes for completion. Comparison of several recorded fusion events indicated that the location of the site of origin was apparently not confined to any particular region along the length of the cell border but was always restricted to the cell apex.

To define the position of the site of origin more precisely in individual cell fusion events, live dual-channel confocal laser scanning microscopy (CLSM) was used to compare the dynamics of both FM 4–64-labeled cell membranes and a fusion protein combining the apical MH27 protein with green fluorescent protein (MH27–GFP). The distribution of MH27 protein defines the apical zonulae adherens of all epithelial cells in *C. elegans* [18], and has been employed to document the developmental timing of hypodermal cell fusions [14,19]. Optical cross-sections clearly showed that MH27–GFP, which was initially found at the apical edge of the prefusion cell border, localized at the receding edge of fusing cell membranes, such that the

Figure 1

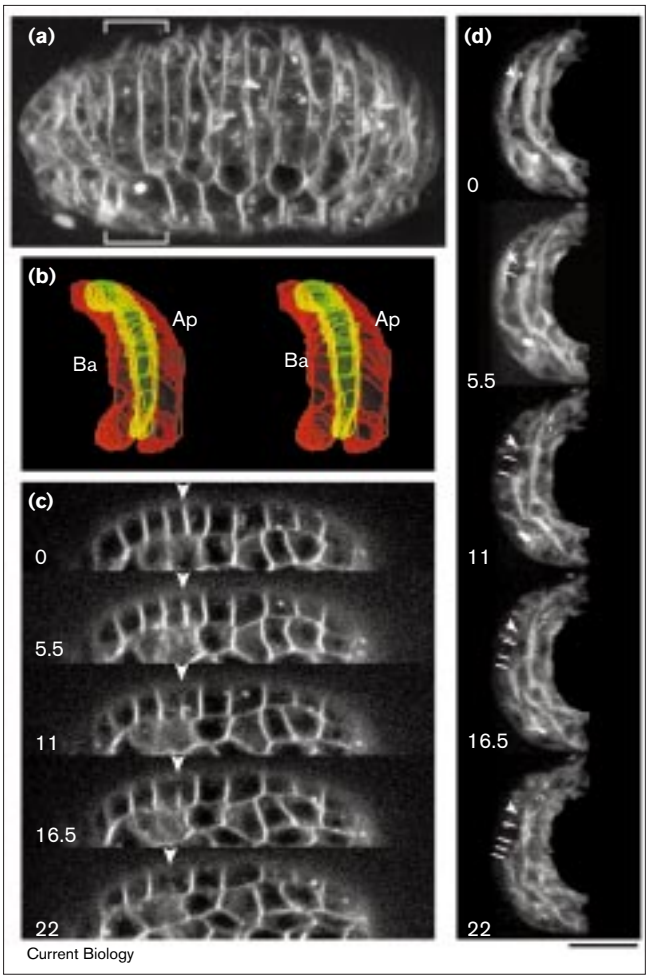

Live MPLSM imaging of hypodermal cell fusions. (a) Three-dimensional reconstruction of the hypodermis of a prefusion embryo labeled with FM 4–64 and viewed dorsolaterally. This projection, comprising 30 serial 0.5 μm-spaced MPLSM sections through half of the embryo, has been 'cored' to eliminate interfering data from deep embryonic structures [17]. Dorsal cells run vertically to the top of the image. Brackets show the region depicted in isolation in (d). (b) Computer reconstruction showing the geometry of hyp7 precursors shortly before fusion. Stereo image of three adjacent dorsal precursors from (a) reconstructed in isolation and false-colored (red, green, red). Lateral cell borders which fuse appear yellow; apical (Ap) and basal (Ba) surfaces are convex and concave, respectively. (c) Cell fusion proceeds in an apical-to-basal direction. Time sequence showing disappearance of lateral membranes (arrowhead) in an optical cross-section through a pair of fusing cells. (d) The fusion aperture propagates from a single apical origin. Time sequence of a cored stereo-four-dimensional reconstruction of a fusing cell border from the embryo in (a), rotated left 45° about the y-axis. Note the semi-elliptical opening at 5.5 min. The origin (arrowhead) and progress (tickmarks) of the opening in one direction are marked along the length of the cell border. Times shown in (c,d) are in min. The scale bar represents 10 μm.

Figure 2

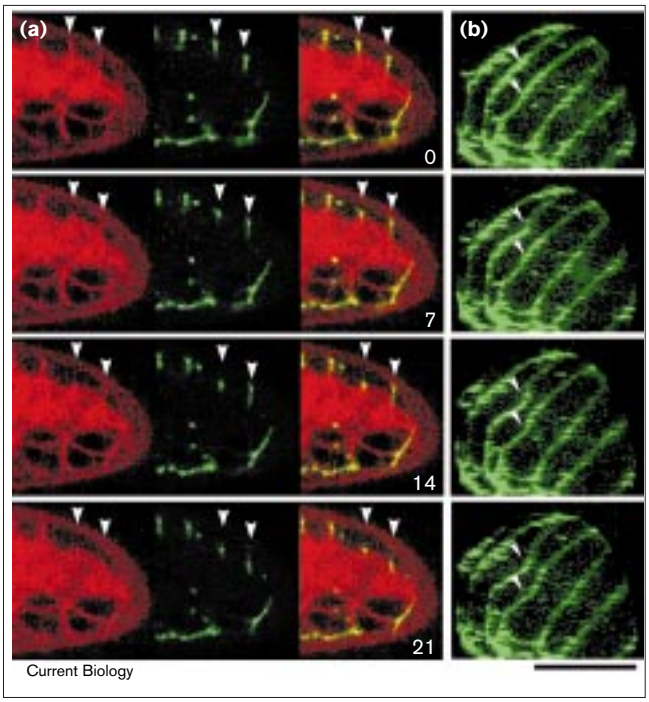

Displacement of the apical adherens junction by cell fusion. (a) MH27–GFP associates with the receding edge of fusing lateral membranes. CLSM time sequence of an optical section through three fusing cells. MH27–GFP (green, center) and FM 4–64 (red, left) were imaged simultaneously; the merged image is shown in the panels on the right. Arrowheads indicate fusing cell borders. (b) MH27–GFP relocalizes in a wavelike manner. Stereo-four-dimensional reconstruction of MH27–GFP from the same embryo, depicting projections rotated left 45° about the y-axis. Arrowheads indicate fusions seen in (a). Times are shown in min. The scale bar represents 10 μm.

junctional protein was separated from the apical membrane of the syncytium by the widening fusion aperture (Figure 2a). Thus, once the fusing lateral membranes had sunk to the full depth of the cells, MH27–GFP was actually basally localized. Dissolution of the MH27 signal between cells occurred only after membrane fusion and displacement of the junction, usually within 5 to 10 minutes. Stereo-four-dimensional reconstruction revealed that the movement of the junctional marker, like the fusion of the membranes themselves, started at a single site and propagated as a wave along the length of the fusing cells (Figure 2b). We conclude that the initiation site for cell fusion resides either within the junction itself or immediately apical to the adherens junction.

To address the means by which the membranes between fusing cells withdraw, we recorded embryos by MPLSM and then immediately fixed them for transmission electron microscopy (TEM). Cell fusions whose early stages were recorded live were thus caught in an intermediate state for ultrastructural examination (Figure 3). In serial TEM sections, the directional spreading of the fusion aperture was again apparent. At the receding edge of the fusing lateral border, a continuous coplanar fringe of irregularly sized

Figure 3

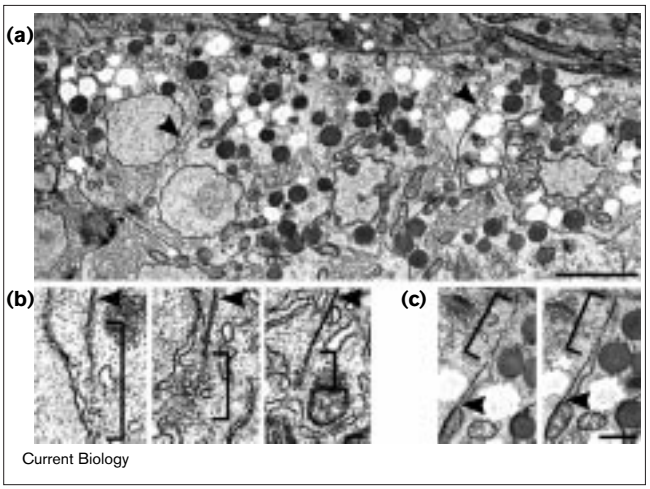

Vesiculation of membranes at the leading edge of the fusion aperture. (a) TEM of an embryo fixed while two cell fusion events were in progress (arrowheads). The scale bar represents 2 μm. (b) Serial cross-sections through the leftmost fusing cell border in (a) shown at higher magnification. The arrowhead marks the region of intact membrane. The bracket indicates the zone of vesiculation. The spacing between sections is ~300 nm. The scale bar represents 100 nm. (c) Tangential sections through the vesiculating zone of the rightmost fusing border in (a). The spacing between sections is ~70 nm. The scale bar represents 500 nm.

Figure 4

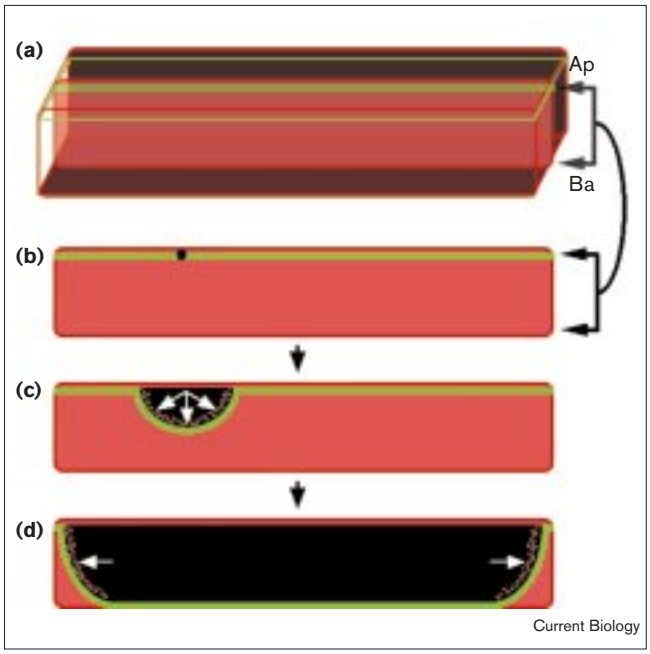

Model for initiation and spreading of the fusion aperture. (a) Idealized representation of two adjacent hypodermal precursor cells. Cell membranes are shown in red, the adherens junctions in green. (b) A single original pore (black spot) forms within or apical to the junction. (c,d) The opening widens, displacing the junction and producing a fringe of vesiculated membrane at the leading edge of the hole. In (b–d), the common border between cells is shown alone within the plane of the page.

vesicles (10–50 nm in diameter) extended 200–600 nm into the growing opening. Beyond this zone of vesiculation, however, intact membrane reached the limit of the cell without interruption.

In summary, fusion commences at a single point within a slim apical subregion of the cell–cell interface, and slowly opens by a process involving vesiculation of the double bilayer and migration of junctional components to the basal surface of the resulting syncytium (Figure 4). A focal origin is consistent with the notion of a virus-like pore. Yet expansion of the opening occurs not merely by unfolding and flow of the contiguous apposed bilayers — the topologically and energetically simplest approach — but also by internalization of the plasma membranes, perhaps to accommodate the reduced surface:volume ratio requirements of the syncytium. Thus, fusion entails specific localization of a vesiculating activity to the rim of the growing hole in the membranes. Association of junctional proteins with the retreating edge of the septal border between fusing cells suggests that the vesiculating activity may associate with the junctional complex throughout the fusion process. Such a complex might resemble or share components with those involved in other forms of endocytosis or acting on similar tightly bent double-bilayers within intracellular organelles [20,21].

These experiments are the first to detail the course of a developmental cell fusion event through direct observation of the fusing cell membranes, and our results should have relevance for other instances of developmental syncytiogenesis. Several other fusing cell types develop stable or transient intercellular junctions before fusion occurs and may use these junctions to organize the fusion mechanism [2,13]. Recently, diverse genes from several organisms have been reported to have roles in cell fusion [6,7,13,22–26]. Understanding the timing and structure of the cellular intermediates in this carefully orchestrated process should point the way to specific functions for the molecules involved.

Materials and methods

Live fluorescence microscopy

MPLSM was used for most recordings to maximize spatio-temporal resolution and embryo viability while minimizing photobleaching, and was performed using a femtosecond-pulsed 1047 nm Nd:YLF laser on a microscope previously described [27]. Cell membranes fluoresced in the presence of 10 μg/ml FM 4–64 (Molecular Probes). CLSM was performed on a Bio-Rad MRC600 to take advantage of dual-channel imaging capabilities not currently available on this MPLSM system. Laser-permeabilized embryo culture, automated image collection, four-dimensional animation, and stereo-four-dimensional reconstruction were performed as previously described using adaptations of published techniques [16,17].

Construction of MH27–GFP

A bright mutant of GFP (S65A, V68L, S72A) [28] was fused to the predicted carboxyl terminus of MH27 by ligation with a genomic fragment

containing the MH27 gene, and the transgene construct was stably integrated into the genome of wild-type worms to create the strain jcls1 (J.S.S. and J.D.H., unpublished). Transgenic worms were phenotypically normal, and the temporal expression and localization of the fluorescent protein faithfully recapitulated those of the endogenous MH27 antigen as detected by immunofluorescence [14,18,19].

Correlative electron microscopy

Live-imaged embryos attached to a poly-L-lysine coated coverslip were fixed by room temperature incubation of the coverslip for 45 min in 1% OsO_4, 0.8% $K_3Fe(CN)_6$, 0.1 M cacodylate buffer, pH 6.0, followed by rinsing in 0.05 M cacodylate buffer, pH 7.0, and incubation for 15 min in 0.2% tannic acid, 0.05 M cacodylate buffer, pH 7.0. This osmium-based fixation protocol was used specifically to avoid membrane artifacts which commonly result from aldehyde fixation [29,30]. Fixed embryos were dehydrated through an acetone series, and embedded in Epon/Araldite while still attached to the coverslip. Glass was dissolved with hydrofluoric acid to yield a flat face for sectioning which was parallel to the plane of optical sections in the MPLSM recording.

Supplementary material

Movies of the data shown in Figures 1 and 2 are published with this paper on the internet.

Acknowledgements

We thank D. Wokosin and V. Centonze-Frohlich for assistance with microscopy. This work was supported by NIH grants GM52454 to J.G.W. and RR00570 to the Integrated Microscopy Resource; by a Lucille P. Markey Award in the Biomedical Sciences and a NSF Young Investigator Award to J.D.H.; by NIH fellowship GM18200-02 to W.A.M.; and by NIH Gamete and Embryo Biology Training Grant HD07342-08 and a Helen Hay Whitney Foundation fellowship to J.S.S.

References

1. Capers CR: Multinucleation of skeletal muscle ***in vitro***. *J Biophys Biochem Cytol* 1959, 7:559-566.
2. Pierce GP, Midgely ARJ: The origin and function of human syncytiotrophoblastic giant cells. *Am J Pathol* 1963, 43:153-173.
3. Sutton JS, Weiss L: Transformation of monocytes in tissue culture into macrophages, epithelioid cells, and multi-nucleated giant cells: an electron microscopic study. *J Cell Biol* 1966, 28:303-332.
4. Sulston JE, Schierenberg E, White JG, Thomson JN: The embryonic cell lineage of the nematode ***Caenorhabditis elegans***. *Dev Biol* 1983, 100:64-119.
5. Ball EE, Goodman CS: Muscle development in the grasshopper embryo: II. Syncytial origin of the extensor tibiae muscle pioneers. *Dev Biol* 1985, 111:399-416.
6. Blobel CP, Wolfsberg TG, Turck CW, Myles DG, Primakoff P, White JM: A potential fusion peptide and an integrin ligand domain in a protein active in sperm–egg fusion. *Nature* 1992, 356:248-252.
7. Yagami-Hiromasa T, Sato T, Kurisaki T, Kamijo K, Nabeshimi Y, Fujisawa-Sehara A: A metallprotease-disintegrin participating in myoblast fusion. *Nature* 1995, 377:652-656.
8. Hernandez LD, Hoffman LR, Wolfsberg TG, White JM: Virus–cell and cell–cell fusion. *Annu Rev Cell Dev Biol* 1996, 12:627-661.
9. Spruce AE, Iwata A, White JM, Almers W: Patch clamp studies of single cell-fusion events mediated by a viral protein. *Nature* 1989, 342:555-558.
10. Zimmerberg J, Blumenthal R, Sarkar DP, Curran M, Morris SJ: Restricted movement of lipid and aqueous dyes through pores formed by influenza hemagglutinin during cell fusion. *J Cell Biol* 1994, 127:1885-1894.
11. Plonsky I, Zimmerberg J: The initial fusion pore induced by baculovirus GP64 is large and forms quickly. *J Cell Biol* 1996, 135:1831-1839.
12. Kalderon N, Gilula NB: Membrane events involved in myoblast fusion. *J Cell Biol* 1979, 81:411-425.
13. Doberstein SK, Fetter RD, Mehta AY, Goodman C: Genetic analysis of myoblast fusion: blown fuse is required for progression beyond the prefusion complex. *J Cell Biol* 1997, 136:1249-1261.
14. Podbilewicz B, White JG: Cell fusions in the developing epithelia of ***C. elegans***. *Dev Biol* 1994, 161:406-424.
15. Denk W, Strickler JH, Webb WW: Two-photon laser scanning fluorescence microscopy. *Science* 1990, 248:73-76.
16. Thomas C, DeVries P, Hardin J, White J: Four-dimensional imaging: computer visualization of 3D movements in living specimens. *Science* 1996, 273:603-607.
17. Mohler WA, White JG: Stereo-4-D reconstruction and animation from living fluorescent specimens. *BioTechniques* 1998, 24:1006-1012.
18. Waterston RH: Muscle. In *The Nematode* Caenorhabditis elegans. Edited by Wood WB. Cold Spring Harbor: Cold Spring Harbor Laboratory Press; 1988:281-335.
19. Priess JR, Hirsh DI: ***Caenorhabditis elegans*** morphogenesis: the role of cytoskeleton in elongation of the embryo. *Dev Biol* 1986, 117:156-173.
20. Riezman H, Woodman PG, van Meer G, Marsh M: Molecular mechanisms of endocytosis. *Cell* 1997, 91:731-738.
21. Jones SM, Howell KE, Henley JR, Cao H, McNiven MA: Role of dynamin in the formation of transport vesicles from the trans-Golgi network. *Science* 1998, 279:573-577.
22. Elion EA, Trueheart J, Fink GR: Fus2 localizes near the site of cell fusion and is required for both cell fusion and nuclear alignment during zygote formation. *J Cell Biol* 1995, 130:183-1296.
23. Trueheart J, Fink GR: The yeast cell fusion protein FUS1 is O-glycosylated and spans the plasma membrane. *Proc Natl Acad Sci USA* 1989, 86:9916-9920.
24. Paululat A, Goubeaud A, Damm C, Knirr S, Burchard S, Renkawitz-Pohl R: The mesodermal expression of rolling stone (rost) is essential for myoblast fusion in Drosophila and encodes a potential transmembrane protein. *J Cell Biol* 1997, 138:337-348.
25. Erickson MR, Galletta BJ, Abmayr SM: Drosophila myoblast city encodes a conserved protein that is essential for myoblast fusion, dorsal enclosure, and cytoskeletal organization. *J Cell Biol* 1997, 138:589-603.
26. Philips J, Herskowitz I: Osmotic balance regulates cell fusion during mating in Saccharomyces cerevisiae. *J Cell Biol* 1997, 138:961-974.
27. Wokosin DL, Centonze VE, White JG, Hird SN, Sepsenwol S, Malcolm GPA, *et al.*: Multiple-photon excitation imaging with an all-solid-state laser. *Proc Optic Diag Liv Cell Biofl SPIE* 1996, 2678:38-49.
28. Cormack BP, Valdivia RH, Falkow S: FACS-optimized mutants of the green fluorescent protein (GFP). *Gene* 1996, 173:33-38.
29. Eggli P, Graber W: Improved ultrastructural preservation of rat ciliary body after high pressure freezing and freeze substitution: a perspective view based upon comparison with tissue processed according to a conventional protocol or by osmium tetroxide/microwave fixation. *Microsc Res Tech* 1994, 29:11-22.
30. Morgenstern E: Aldehyde fixation causes membrane vesiculation during platelet exocytosis: a freeze-substitution study. *Scanning Microsc* 1991, Supplement 5:S109-S115.

Supplementary material

Dynamics and ultrastructure of developmental cell fusions in the *Caenorhabditis elegans* hypodermis

William A. Mohler, Jeffrey S. Simske, Ellen M. Williams-Masson, Jeffrey D. Hardin and John G. White

Current Biology 14 September 1998, **8**:1087–1090

Movie 1

Animated rendering of the data from Figure 1. MPLSM focal series of optical sections through an FM 4–64-labeled embryo. Three-dimensional reconstruction, and 'coring' of the embryo shown in Figure 1a. Rotational animation of the false-colored computer reconstruction shown in Figure 1b. Animation of the optical section timecourse from Figure 1c. Stereo-view animation of the stereo-four-dimensional timecourse from Figure 1d.

Movie 2

Animated rendering of the data from Figure 2. Dual channel CLSM focal series through embryo showing FM 4–64 (red) and MH27–GFP (green). Animation of optical section timecourse from Figure 2a showing both channels merged and then each separately. Rotational and timecourse animation of the stereo-four-dimensional reconstruction of MH27–GFP from Figure 2b.